

Device-Free Electromagnetic Passive Localization Using Link Line Information in Wireless Sensor Networks

Li Li¹, Wei Ke^{2, 3, 4, *}, Xiunan Zhang², Yanan Yuan², and Jianhua Shao²

Abstract—The electromagnetic passive localization without the need of carrying any device, named device-free passive localization (DFPL) technique, is an emerging technology for determining an uncooperative target's position. The DFPL technique detects the shadowed links in a monitored area and realizes localization with the received signal strength (RSS) measurements of these links. However, most current RSS-based DFPL schemes belong to the model-based DFPL method, since the localization accuracy depends on the shadowing model. Moreover, model-based DFPL methods require high memory and computing resources for accurate tracking performance, and thus may not be suitable for resource-constrained applications. To overcome these problems, in this paper we propose a lightweight DFPL method which makes use of recent link lines detected by wireless sensor networks to estimate the target's location. This method can be independent of the shadowing model and can also reduce the algorithm's storage and computational resource requirements. The effectiveness and robustness of the proposed scheme are demonstrated by experimental results where the proposed algorithm yields substantial improvement for localization performance and complexity.

1. INTRODUCTION

Wireless localization and tracking have gained considerable attention over the past decade, as location-awareness is becoming a basic requirement in both industry and everyday life. Generally, the localization research area can be divided into active and passive localizations. While the active localization technique [1, 2] that equips the target with a wireless device like a smartphone or a RFID tag has been widely studied, the passive localization technique, which could realize device-free localization, is still an emerging and challenging technique. In recent years, the low-cost DFPL which only utilizes RSS measurements of wireless links has become an attractive technology and shown enormous promise in applications ranging from intrusion detection to elder care [3, 4]. The basic principle of RSS-based DFPL is that when a target moves into the area within a wireless network, it may cause the changes of RSS by shadowing, reflecting, diffracting, or scattering. The shadowed links will be different when the target is located at different locations, and this makes it possible to realize DFPL based on the link measurements [3, 4]. Compared with the existing device-free techniques such as infrared detector, video monitor and UWB radar detector, RSS-based DFPL brings several advantages over other technologies by being able to work in obstructed environments, see through smoke, darkness, and walls, while avoiding the privacy concerns raised by video cameras.

Due to potential commercial and military application that can be enriched by DFPL, in recent years lots of research works have been carried out to realize DFPL. Youssef et al. [4, 5] first proposed

Received 4 February 2016, Accepted 14 April 2016, Scheduled 25 April 2016

* Corresponding author: Wei Ke (kewei@njnu.edu.cn).

¹ Department of Mechanical and Electrical Engineering, Nantong College of Science and Technology, Nantong 226007, China.

² Jiangsu Key Laboratory on Optoelectronic Technology in School of Physics and Technology, Nanjing Normal University, Nanjing 210023, China. ³ Jiangsu Center for Collaborative Innovation in Geographical Information Resource Development and Application, Nanjing 210023, China. ⁴ Jiangsu Key Laboratory of Meteorological Observation and Information Processing, Nanjing University of Information Science & Technology, Nanjing 210044, China.

the term of DFPL and realized DFPL with a fingerprint-matching method. They exploited a radio map, constructed by measuring the RSS in predetermined locations of the target or by the radio frequency (RF) propagation model, and then matched the observed RSS to the training data for determining the target's location. As the fingerprinting method used in the device-dependent localization system, however, the training measurements increase exponentially with the increase of the number of wireless links and targets. In addition, this method is also environment dependent, and any significant change on the topology implies a costly new recalibration. Another approach to RSS-based DFPL, named radio tomographic imaging (RTI) [6, 7], estimates the changes in the RF propagation field of the monitored area and then forms an image of the changed field. This image is then used to infer the locations of targets within the deployed network. The drawback of imaging-based DFPL systems is that information can be lost in the two-step process [7]. Due to its excellent performance in signal reconstruction, compressed sensing (CS) has recently been applied to DFPL by exploiting spatial sparsity. Reference [8] carried out the first work to combine spatial sparsity and RTI technology [6] to solve the DFPL problem. In [9, 10], the greedy algorithm was used to estimate targets' positions, which leads to a substantial reduction of the amount of measurements. Reference [11] exploited the dictionary learning technique to adjust the basis matrix for enhancing location accuracy.

In general, all these aforementioned approaches belong to the model-based DFPL method. A key problem in model-based DFPL methods is to construct a reasonable shadowing model in order to accurately relate the shadowing experienced by a signal to attenuation at specific in space. However, so far most shadowing models are only approximate to real radio propagation characters. For example, although the normalized ellipse shadowing (NES) model [6, 12] has some physical justification for using an ellipse shape according to the ellipsoidal Fresnel zone, the decision to set the weights of all of the grids equally in each ellipse and invariably in all environments has no physical basis. In addition, to generate a location estimate model-based DFPL methods need perform operations on large matrices for solving the underdetermined problem which results in high storage and computing requirements.

Different from the model-based methods, Zhang et al. [13, 14] first proposed the geometric-based DFPL method and further explored by Hillyard et al. [15]. Instead of exploiting the shadowing model, the geometric-based DFPL method detects the wireless link line information affected by targets to realize DFPL. Since the geometric-based method does not need solve the underdetermined problem, it can reduce the storage and computational requirements, resulting in fast execution times. In this paper, we continue to investigate the geometric-based DFPL method by exploiting the prior location information to remove outlier links and improbable target locations. The remainder of the paper is organized as follows. Section 2 describes the problem formulation. In Section 3, we propose a novel geometric-based DFPL method by utilizing the prior information to improve tracking performance. Experimental results are given in Section 4. Finally, Section 5 concludes the paper.

2. PROBLEM FORMULATION

Suppose that M wireless nodes with known locations consist of the wireless network, and then the total number of wireless links with every pair of nodes is $K = M \times (M - 1)/2$. Here, any pair of nodes is counted as a link, whether or not communication actually occurs between them. When wireless nodes communicate, the radio signals pass through the physical area of the network. Thus, the target's presence inside the monitored region causes changes in the RSS of a subset of these K links due to scattering, reflection, diffraction or absorption. Although these effects can be regulated by certain physical principle in theory, it is difficult to describe the multipath propagation of electromagnetic waves in practice. Therefore, the semi-empirical propagation model is widely adopted to approximate the signal propagation character [6, 12]. With the semi-empirical model in [6, 12], the measurement $y_i(t)$ of link i is described as

$$y_i(t) = P_i - J_i - S_i(t) - F_i(t) - v_i(t) \quad (1)$$

where P_i is the transmitted power in dBm, $S_i(t)$ the shadowing loss in decibels due to targets that attenuate the signal, $F_i(t)$ the fading loss in decibels, and J_i the static losses in decibels due to distance, antenna patterns, device inconsistencies, etc., and $v_i(t)$ represents noise and interference. At time t , the change of the RSS measurement $y_i(t)$ is

$$\Delta y_i(t) = y_i(t) - y_i(0) \approx -S_i(t) - v_i(t) + v_i(0) \quad (2)$$

where $y_i(0)$ is the baseline RSS measurement that can be learned offline from the link measurements when the deployment area is vacant or that can be learned online with the method proposed in [16]. Generally, measurement noises $v_i(t)$ and $v_i(0)$ are negligible compared with the shadowing loss. Hence, $y_i(t)$ is primarily determined by the shadowing loss at time t .

Model-based methods such as RTI [6] and CS-DFPL [8] divide the network deployment area into N grids and use the NES model to assign weights to each grid. Non-zero weights are assigned to grids that lie within the path defined by an ellipse with foci at each node of the shadowed link. Then, an ill-posed inverse problem is solved by the regularized least-squares approach in RTI or by CS reconstruction algorithm in CS-DFPL to obtain an image of the deployment area. Grids in the obtained image with significant attenuation represent possible locations of the target. While model-based methods achieve reasonable tracking accuracy, a main drawback of these methods is that a large number of grids ($N > 1000$) is typically required to overcome the inherent quantization error. Since model-based DFPL methods usually require the construction of weight matrices [6–10] or shadowing effect maps [4, 5], these methods must maintain a $K \times N$ matrix. Hence, these model-based methods may be unsuitable for memory-limited applications. Moreover, in order to obtain a target's location, model-based methods need perform operations on large weight matrices and thus require high computing resources. In addition, since the NES model is only approximate to the real RF propagation, the weighting values are not very accurate for reconstruction, especially in multipath environments.

In view of the above limitation, in this paper we propose a lightweight geometric-based DFPL method which is independent of approximate weighting model. The proposed method only exploits recent link lines detected by wireless sensor networks to estimate the target's location and thus reduces the algorithm's storage and computational requirements. Moreover, unlike geometric-based DFPL methods in [13–15], the proposed method makes use of prior information to improve the tracking results, making it more robust to noise.

3. GEOMETRIC-BASED DFPL ALGORITHM WITH PRIOR INFORMATION

In general, the target-affected links tend to intersect with each other at points near the target's true location. Based on this fact, we propose a new geometric-based DFPL (GDFPL) algorithm which makes use of link line information to estimate the target's location for avoiding model errors. It consists of three main steps: detecting the affected links, outlier link rejection, and triangle localization.

3.1. Detecting the Affected Links

The RSS measurement $y_i(t)$ of a link L_i is defined as the RSS measurement from one end node to another. When all K links in the network are considered, let $\mathbf{Y}(t) = [y_1(t)y_2(t) \dots y_K(t)]$ be the vector of RSS measurements for all links at time t . Correspondingly, $\mathbf{Y}(0) = [y_1(0)y_2(0) \dots y_K(0)]$ is the vector of baseline RSS measurements for all links.

Many experiments have demonstrated that RSS is particularly sensitive to noise, and the RSS measurements may still vary when the deployment area is vacant. Moreover, in rich multipath environments, a wireless link may experience either attenuation or amplification due to the presence of the target in its vicinity [17]. To determine which links are shadowed by targets, the baseline RSS vector $\mathbf{Y}(0)$ is subtracted from the current RSS vector $\mathbf{Y}(t)$ to obtain $\Delta\mathbf{Y}(t)$, i.e., $\Delta\mathbf{Y}(t) = \text{abs}[\mathbf{Y}(t) - \mathbf{Y}(0)]$, where $\text{abs}[\cdot]$ is the operation of absolute value. Thus, a link i is considered to be shadowed by the target if its corresponding change in RSS measurement $\Delta y_i(t)$ is above the shadowing detection threshold y_{th} . Define the effective set \mathbf{S}_t of the affected links as

$$\mathbf{S}_t = \{L_i | \Delta y_i(t) > y_{th}\} \quad (3)$$

y_{th} is a user-defined parameter indicating the shadowing detection threshold. Since the detection threshold is usually larger than the RSS variation affected by noise, Eq. (3) can guarantee that the noise influence is alleviated, and only significant link components are selected

3.2. Outlier Link Rejection

Although the noise influence to wireless links is reduced by using Eq. (3), not all of the detected effective links go through the vicinity of the target. Many experiments have found that the changes of RSS in some wireless links that are far from the target can also be above the shadowing detection threshold due to multipath effects. If such outlier links are included to generate a location estimate, tracking errors will become large because they may intersect with other effective links at points far away from the target. In order to eliminate the effect of these outlier links, we make use of the prior location information to select the links that are really affected by the target. Nonetheless, in DFPL applications this prior information is not easy to obtain, since the target to be tracked is generally uncooperative. Moreover, not only are the speed and direction of the target unknown, but also the accurate motion model of the target is unavailable in most cases. The only information about the target that is available to a DFPL system is its previous location estimate and the assumption that the target's maximum speed is below a threshold u_{\max} . To make the algorithm as universal as possible, the prior region \mathbf{z}_t is defined as a circle centered on the previous target location estimate

$$\mathbf{z}_t = \{\mathbf{p}_t | H(\mathbf{p}_{t-1}, \mathbf{p}_t) < r\} \quad (4)$$

where $\mathbf{p}_{t-1} = [x_{t-1}, y_{t-1}]$ is the previous location coordinate; \mathbf{p}_t is the coordinate of a point inside the deployment area; $H(\mathbf{p}_{t-1}, \mathbf{p}_t)$ is the Euclidean distance between the locations \mathbf{p}_{t-1} and \mathbf{p}_t ; r is the radius of the circular prior region. The radius r of the prior region is dependent on the maximum distance that the target can travel in the time between sampling instants t , i.e., $r \geq u_{\max} \times t$. As shown in Fig. 1, the predicted prior region \mathbf{z}_t contains the information about which points the target is more likely to be located at. Therefore, shadowed links in \mathbf{S}_t that do not intersect the prior region should be removed.

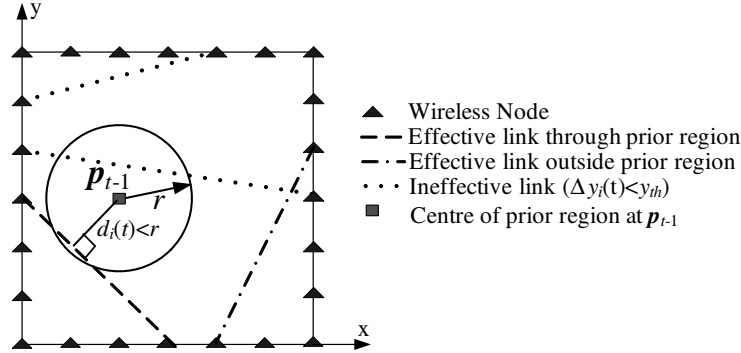


Figure 1. An illustration of the prior region and effective links.

To recognize if a link in \mathbf{S}_t intersects the prior region \mathbf{z}_t , we only need check if the shortest distance between the link and center of the prior region is not greater than radius r . Let the shadowed link i be represented by the line segment L_i from the node at location coordinate $n_i^a = [x_i^a, y_i^a]$ to the node at location coordinate $n_i^b = [x_i^b, y_i^b]$. Thus, the line equation can be represented as $y = k_i x + b_i$, where the slope k_i is $(y_i^b - y_i^a)/(x_i^b - x_i^a)$, and the intercept b_i is $y_i^a - k_i x_i^a$. Then, the shortest distance between the center of the prior region and link i is

$$d_i(t) = \frac{|k_i x_{t-1} - y_{t-1} + b_i|}{\sqrt{1 + k_i^2}} \quad (5)$$

Distance $d_i(t)$ determines whether link i intersects the prior region \mathbf{z}_t . Then, the modified effective set \mathbf{S}'_t of links that intersect the prior region \mathbf{z}_t can be defined as

$$\mathbf{S}'_t = \{L_i | \Delta y_i(t) > y_{th} \& d_i(t) < r\} \quad (6)$$

This means that only when $d_i(t) < r$, link i in \mathbf{S}_t can be added to the new effective set \mathbf{S}'_t and considered for generating the target location estimate.

3.3. Triangle Localization

Generally, after the affected link identification and outlier link rejection, the links in set \mathbf{S}'_t can be considered as real links which have been sufficiently influenced by the presence of the target. In the LLC algorithm [15], the affected links in the network are represented as line segments, and then the LLC algorithm uses ordinary least squares (LS) to estimate the intersection points of these line segments. Different from applying LS method to estimate intersection points in [15], in this paper we seek to find a pivot point by forming virtual triangles consisting of links. We choose any three links out of \mathbf{S}'_t to form a virtual triangle. Assuming that there are Q ($Q < K$) links in \mathbf{S}'_t , there will be maximum Σ_{\max} ($\Sigma_{\max} \leq \binom{Q}{3}$) number of triangles, and each triangle yields a centroid location. We define the pivot point (x_t, y_t) as the weighted average of all the triangle centroids:

$$x_{pivot} = \frac{\sum_j^{\Sigma_{\max}} \omega_j x_j}{\sum_j^{\Sigma_{\max}} \omega_j}, \quad y_{pivot} = \frac{\sum_j^{\Sigma_{\max}} \omega_j y_j}{\sum_j^{\Sigma_{\max}} \omega_j} \quad (7)$$

where (x_j, y_j) is the centroid of the j th virtual triangle; ω_j is the weight of the triangle and equals the sum of RSS changes $y_i(t)$ of three links forming the triangle. Thus, higher weights are assigned to centroids of triangles that are constructed by more heavily shadowed links. This is in accord with the fact that the target is more likely to be in the path of heavily shadowed links. Fig. 2 depicts the scenario of obtaining the pivot point by weighted average of the centroid of three triangles.

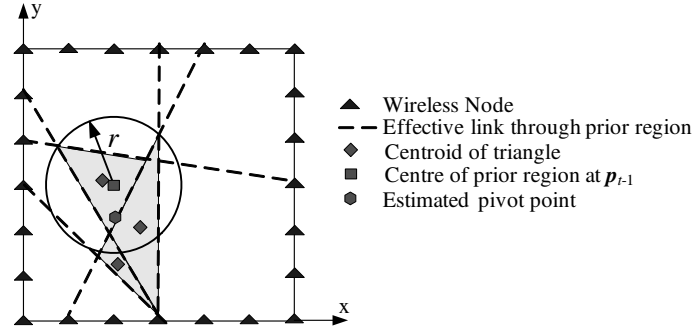


Figure 2. An illustration of triangle localization.

However, it should be noted that some centroids of triangles may lie outside the circular prior region. Since each centroid represents a possible location of the target at time t , centroids that lie outside the circular prior region may have low possibility to be the true location of the target. Based on the above analysis, we utilize the circular spatial filter again to assign the possibility p_j to the centroid j as

$$p_j = \begin{cases} 1, & \text{if } H(\mathbf{p}_{t-1}, c_t^j) < r \\ 0, & \text{otherwise} \end{cases} \quad (8)$$

where c_t^j represents the location of j th centroid at time t , and $H(\mathbf{p}_{t-1}, c_t^j)$ is the Euclidean distance between locations \mathbf{p}_{t-1} and c_t^j . After calculating possibility p_j for each centroid, the modified location estimate of the target is

$$x_{pivot} = \frac{\sum_j^{\Sigma_{\max}} p_j \omega_j x_j}{\sum_j^{\Sigma_{\max}} p_j \omega_j}, \quad y_{pivot} = \frac{\sum_j^{\Sigma_{\max}} p_j \omega_j y_j}{\sum_j^{\Sigma_{\max}} p_j \omega_j} \quad (9)$$

4. EXPERIMENTAL RESULTS

4.1. Physical Description of the Experiment

To evaluate the performance of the proposed algorithm, we performed extensive experiments based on a wireless sensor network in an uncluttered outdoor environment (Scene 1) and a highly cluttered indoor environment (Scene 2). In both environments, the wireless nodes are placed at the monitored region's perimeter, and each node is 1 m off the ground on a tripod. In Scene 1, twenty-four wireless nodes were placed 1 m apart at the perimeter of an 6 m \times 6 m area, while twenty two wireless nodes were deployed to form a 6 m \times 5 m area in Scene 2. Photographs of the experimental setup are shown in Fig. 3. In both scenes, a base-station node listens to all broadcasts from the perimeter nodes and logs the RSS information to a mobile computer with 3.1 GHz processor and 4 GB memory for real-time processing. In this paper, we assume that there is only a single target to be tracked. In addition, in the experiments we assume that the starting location of the target is known, which is commonly used in many target tracking algorithms.

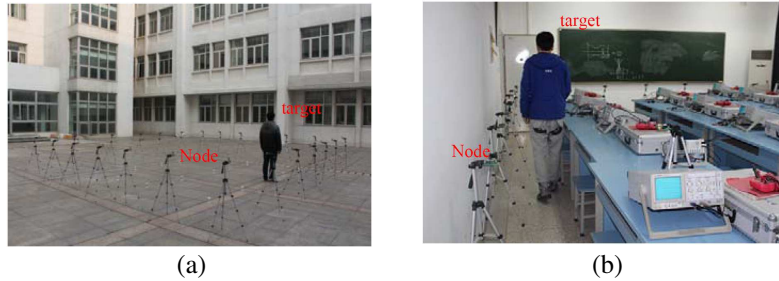


Figure 3. The photographs of two experimental scenes. (a) Scene 1. (b) Scene 2.

The transceivers of the nodes are system-on-chip (SoC) CC2530 devices; each node has a monopole antenna and uses the 24 GHz IEEE 802154 standard for communications. To avoid network transmission collisions, a simple token ring protocol is used to control transmission. Each node is assigned an ID number and programmed with a known order of transmission. When a node transmits, each node that receives the transmission examines the sender identification number and reserves the RSS from the transmitting node. The receiving nodes check to see if it is their turn to transmit, and if not, they wait for the next node to transmit. If one node does not transmit, or the packet is corrupted, a timeout causes each receiver to move to the next node in the schedule so that cycle is not halted. To obtain the baseline RSS, measurements were taken for 60 s while the single human target is outside the deployment area. Afterwards, a target walked inside the deployment area along a predefined trajectory. The default parameters are as follows: the detection threshold $y_{th} = 3$ dB, the radius of prior region $r = 1.0$ m and the true speed of the target is about 1 m/s. The tracking error is defined as the distance between the known true target location and the estimated location obtained by each algorithm. To achieve reliable results, all the statistical results are the average of 30 repeated experiments with independent measurement data for high confidence.

4.2. Performance Analysis and Comparison

The tracking trajectories along the predefined path obtained by the proposed method are shown in Figs. 4(a) and (b), respectively. From Fig. 4, we can find that the proposed GDFPL approach can track the target's motion well whether the tracking trajectory is the square path or the S-curve path. Even in the presence of multiple obstructions in Scene 2, the proposed algorithm can still track the target with meter-level accuracy. Meanwhile, Fig. 4 also indicates that the tracking errors at the four corners are relatively larger than the others. This phenomenon is mainly due to the fact that when the target changes direction, some transient error will occur while the variations of wireless links traveling through the target are abrupt and discontinuous.

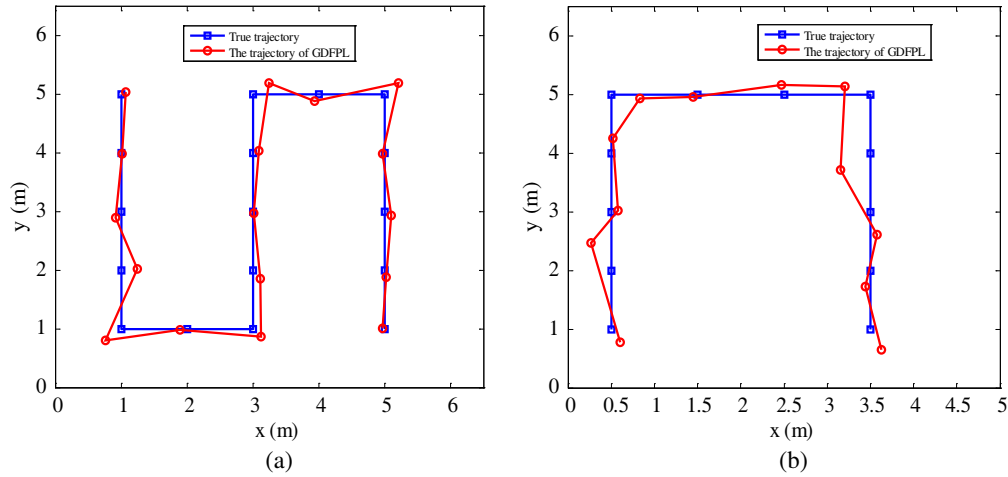


Figure 4. The tracking results along the path. (a) Scene 1. (b) Scene 2.

Then, we compared the GDFPL method with two state-of-the-art DFPL schemes, i.e., the geometric-based LLC algorithm in [15] and the model-based RTI algorithm in [6] under the same conditions. In the RTI method, the width of the ellipse is set as 0.3 m, and grid size is 0.25 m × 0.25 m. Tables 1(a) and (b) summarize the statistical results of tracking errors in both scenes, respectively. We can find that due to the full utilization of the space-domain prior information of the location vector, the GDFPL algorithm achieves better performance than the other algorithms. Compared with that of the LLC and RTI algorithms, in Scene 1 the mean tracking error of the GDFPL algorithm reduces 39.8% and 41.7%, respectively. Meanwhile, we can see that although the mean values of the tracking errors in three schemes are all less than 1 m, the proposed approach has significantly better performance than the other two methods in terms of RMSE. For Scene 2, the tracking errors become larger for all algorithms due to the challenging indoor environment. Nevertheless, the GDFPL algorithm can perform the best tracking performance with less than 1 m mean error. This means that applying the threshold y_{th} and the prior region can effectively remove outlier links in multipath environments and enhance the localization stability of DFPL.

Table 1. Comparisons of localization error and running time in both scenes. (a) Scene 1. (b) Scene 2.

Algorithm	Mean (m)	RMSE (m)	Running Time (ms)	Algorithm	Mean (m)	RMSE (m)	Running Time (ms)
GDFPL	0.56	0.63	9.55	GDFPL	0.85	0.95	9.68
LLC	0.93	1.08	9.23	LLC	1.77	1.39	9.81
RTI	0.96	1.61	95.67	RTI	1.53	2.18	98.13

The complexity is also compared in terms of the CPU running time. From Tables 1(a) and (b), in both scenes each algorithm has nearly equivalent average running time, respectively. Since two geometric-based methods make use of geometric relationship to eliminate the need for storing and processing large matrices, they have significantly faster execution times. In contrast, the model-based RTI method need perform operations on large matrices for solving the underdetermined problem which results in more computing times. Although the proposed GDFPL algorithm and LLC method have identical execution times, the proposed algorithm performs better tracking results in terms of RMSE in the cluttered indoor environment.

Furthermore, we evaluate the GDFPL scheme under different parameters to analyze its performance. Firstly, the performance of the GDFPL algorithm is evaluated under different y_{th} values.

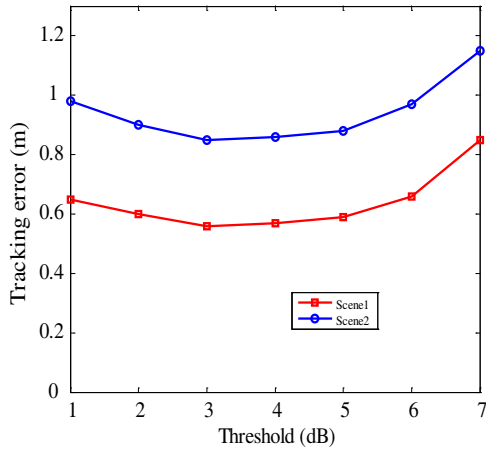


Figure 5. Performance under different detection thresholds.

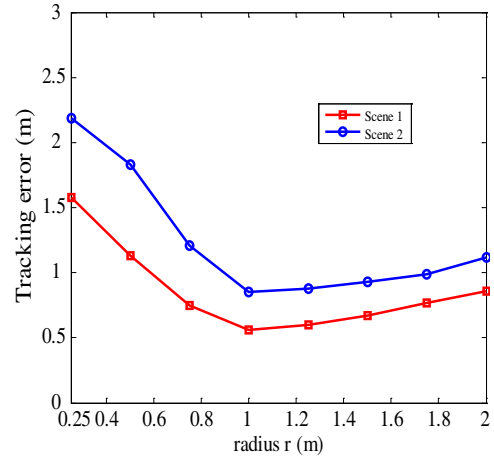


Figure 6. Effects of the different radius of the circular prior region.

From Fig. 5, it can be found that selecting a very high value for y_{th} results in large tracking errors. This is because a too high y_{th} value will yield fewer detected effective links, resulting in fewer centroids with which to estimate the target's true location. On the other hand, setting the value of y_{th} too low makes the proposed algorithm more susceptible to noise, especially in cluttered indoor environments.

The performance of the proposed scheme with different radii of the circular prior region is shown in Fig. 6. Radius r of the prior region has an effect on the outlier link rejection. We can see that setting the value of r too high or too low results in an increase in the tracking error. As defined by Eq. (4), the predicted prior region \mathbf{z}_t is primarily determined by r . When r is too small, the target will move outside the prior region, which results in the misuse of the prior information and then unsatisfactory localization performance. On the other hand, an overlarge value of r will result in the failure to remove outlier links, and the performance will also drop.

5. CONCLUSION

DFPL is a new and promising localization method for non-cooperative objects and can provide the capability of tracking entities not carrying any devices nor participating actively in the localization process. To achieve satisfactory tracking performance and low computing complexity synchronously, a lightweight DFPL method which makes use of recent line crossings detected by the networks' links to estimate the target's location has been proposed. In the proposed algorithm, the links shadowed by the target are treated to form virtual triangles whose centroids are considered as probable target locations. To overcome the negative effect of outlier links, shadowed links that are outside a circular prior region centered on the previous location estimate are removed. A target location estimate is made by fusing the centroids using a weighted mean approach, with weights derived from the shadowing experienced by the effective links that form a virtual triangle. The effectiveness of the proposed scheme has been demonstrated by experimental results in both indoor and outdoor environments where substantial improvement for localization performance and computing complexity is achieved. Future work will emphasize on the theoretic bound on the location estimation precision and extend the proposed algorithm for use in multi-target tracking.

ACKNOWLEDGMENT

This work was supported by the Specialized Research Fund for the Doctoral Program of Higher Education of China (Grant No. 20133207120007), and the Open Research Fund of Jiangsu Key Laboratory of Meteorological Observation and Information Processing (Grant No. KDXS1408).

REFERENCES

1. Mitilineos, S. A. and S. C. A. Thomopoulos, "Positioning accuracy enhancement using error modeling via a polynomial approximation approach," *Progress In Electromagnetics Research*, Vol. 102, 49–64, 2010.
2. Mitilineos, S. A., D. M. Kyriazanos, and O. E. Segou, "Indoor localization with wireless sensor networks," *Progress In Electromagnetics Research*, Vol. 109, 441–474, 2010.
3. Patwari, N. and J. Wilson, "RF sensor networks for device-free localization: measurements, models, and algorithms," *Proc. of the IEEE*, Vol. 98, No. 11, 1961–1973, 2010.
4. Youssef, M., M. Mah, and A. Agrawala, "Challenges: device-free passive localization for wireless environments," *13th ACM MobiCom*, 222–229, 2007.
5. Sabek, I., M. Youssef, and A. V. Vasilakos, "ACE: An accurate and efficient multi-entity device-Free WLAN localization system," *IEEE Trans. Mobile Comput.*, Vol. 14, No. 2, 261–273, 2015.
6. Wilson, J. and N. Patwari, "Radio tomographic imaging with wireless networks," *IEEE Transactions on Mobile Computing*, Vol. 9, No. 5, 621–632, 2010.
7. Kaltiokallio, O., M. Bocca, and N. Patwari, "A fade level-based spatial model for radio tomographic imaging," *IEEE Trans. Mobile Comput.*, Vol. 13, No. 5, 1159–1172, 2014.
8. Kanso, M. A. and M. G. Rabbat, "Compressed RF tomography for wireless sensor networks: centralized and decentralized approaches," *Proc. 5th DCOSS*, 173–186, 2009.
9. Yang, Z. Y. K. D. Huang, X. M. Guo, and G. L. Wang, "A real-time device-free localization system using correlated RSS measurements," *EURASIP J. Wireless Commu. Netw.*, Vol. 2013, No. 186, 1–12, 2013.
10. Wang, J., Q. Gao, X. Zhang, and H. Wang, "Device-free localization with wireless networks based on compressing sensing," *IET Commun.*, Vol. 6, No. 15, 2395–2403, 2012.
11. Ke, W., G. Liu, and T. Fu, "Robust sparsity-based device-free passive localization in wireless networks," *Progress In Electromagnetics Research C*, Vol. 46, 63–73, 2014.
12. Hamilton B. R., X. L. Ma, R. J. Baxley, and S. M. Matechik, "Propagation modeling for radio frequency tomography in wireless networks," *IEEE J. Sel. Topics Signal Process*, Vol. 8, No. 1, 43–54, 2014.
13. Zhang, D., J. Ma, Q. Chen, and L. M. Ni, "An RF-based system for tracking transceiver-free objects," *Proc. 5th PerCom*, 135–144, 2007.
14. Zhang, D., K. Lu, R. Mao, Y. Feng, Y. Liu, Z. Ming, and L. Ni, "Fine-grained localization for multiple transceiver-free objects by using RF-based technologies," *IEEE Trans. Parallel Distrib. Syst.*, Vol. 25, No. 6, 1464–1475, 2014.
15. Hillyard, P., S. Daruki, N. Patwari, and S. Venkatasubramanian, "Tracking estimation using link line crossing information in wireless networks" *Proc. GlobalSIP 2013*, 1037–1040, 2013.
16. Zhao Y. and N. Patwari, "Demo abstract: Histogram distance-based radio tomographic localization," *Proc. 11th ACM/IEEE Int. Conf. IPSN*, 129–130, 2012.
17. Kaltiokallio, O., M. Bocca, and N. Patwari, "Enhancing the accuracy of radio tomographic imaging using channel diversity," *Proc. 9th IEEE Int. Conf. MASS*, 254–262, 2012.